Grassmannian Frame Computation via Accelerated Alternating Projections

Bastien MASSION
ICTEAM - UCLouvain
Louvain-la-Neuve, Belgium
bastien.massion@uclouvain.be

Estelle MASSART
ICTEAM - UCLouvain
Louvain-la-Neuve, Belgium
estelle.massart@uclouvain.be

***Abstract*—This paper addresses the approximation of real and complex Grassmannian frames, namely sets of unit-norm vectors with minimum mutual coherence. We recast this problem as a collection of feasibility problems aiming to design frames with given target coherence, that evolves during the execution of the algorithm. The feasibility problems are solved by an accelerated alternating projection algorithm, leveraging a Gram matrix representation of the frames. Numerical experiments indicate that our proposed Targeted coherence with Accelerated Alternating Projection (TAAP) algorithm outperforms state-of-the-art methods regarding the mutual coherence vs computational cost criterion, exhibiting the largest improvement over existing methods when the frame dimension is comparable to the dimension of the ambient space.**

***Index Terms*—Mutual Coherence, Grassmannian frame, line packing, Gram matrix, Accelerated Alternating Projections**

I. Introduction

The *mutual coherence* of a frame captures the largest similarity between the frame's elements. We represent a frame of n elements in a field $\mathbb{F}^m$ (with $\mathbb{F}$ the set of real numbers $\mathbb{R}$ or complex numbers $\mathbb{C}$) by a matrix $F \in \mathbb{F}^{m\times n}$. We focus on finite overcomplete unit frames, i.e., we assume that $2 \leqslant m < n < \infty$ and $\|f_i\| = 1$ for all $1 \leqslant i \leqslant n$, where $\|\cdot\|$ is the Euclidean norm induced by the Euclidean inner product $\langle \cdot, \cdot \rangle$ and f_i the i^{th} column of F. The mutual coherence of a unit frame $F \in \mathbb{F}^{m\times n}$ [1] is given by

$$\mu : \mathbb{F}^{m\times n} \to [0,1] : F \mapsto \max_{1\leqslant i\neq j\leqslant n} |\langle f_i, f_j\rangle| .$$

Grassmannian frames are minimizers of the mutual coherence for a given dimensions-field triplet $(m, n, \mathbb{F})$, i.e., solve the Minimal Mutual Coherence (MMC) problem [2]:

$$\mu^{\mathbb{F}}_{m,n} = \min_{F\in\mathbb{F}^{m\times n}} \mu(F) \qquad \text{s.t. } \|f_i\| = 1,\ 1 \leqslant i \leqslant n. \quad \text{(MMC)}$$

MMC, also known as *Grassmannian packing*, *line packing* or *projective packing*, has gained much attention in recent years due to its large number of applications. For example, a celebrated result in compressive sensing guarantees that sparse signals can be exactly reconstructed when the sparsity level does not exceed a threshold related to the mutual coherence of the dictionary [3], [4]. Grassmannian frames also allow building codes that are optimally robust to erasures in information and coding theory [1], [5] and provide appealing measurements in quantum state tomography [6]–[8].

The study of Grassmannian frames has drawn much attention over the years. Several works derive uniform lower bounds on the minimal mutual coherence for a given dimensions-field triplet $(m, n, \mathbb{F})$ and manage for some triplets to construct frames matching these bounds; see [5], [9]–[11] for an overview. A celebrated example is the set of equiangular tight frames that attain the Welch bound [12], [13]. However, geometric, combinatorial and graph theoretic arguments demonstrate that the optimal value $\mu^{\mathbb{F}}_{m,n}$ strictly exceeds known lower bounds for some specific triplets, see [14]–[16].

Alternatively, a wide variety of works address the (MMC) problem numerically, for example by smoothing the objective function [17]–[19], convexifying the problem [20]–[22], or lifting constraints as penalty terms, turning it into an unconstrained problem [23], [24]. In particular, the very recent IDB method achieves state-of-the-art results for real frames by combining a penalized unconstrained objective minimized through gradient descent with a bisection-based *coherence targeting scheme* [23]. Some works leverage Riemannian Optimization to solve (MMC) on the Grassmannian manifold (hence the name *Grassmannian packing*) [18], [25], while other take inspiration from physical phenomena such as electric repulsion [26] or sphere collisions [2].

Another line of research proposed by Tropp et al. relies on the reformulation of (MMC) in terms of Gram matrices, and addresses it using Alternating Projections (AP) [27]–[31]. While this representation may lead to a computational overhead due to the increased number of variables, we show here that it becomes very competitive when combined with an acceleration technique and a well-chosen coherence targeting scheme. Our proposed Targeted coherence with Accelerated Alternating Projections (TAAP) method matches or outperforms existing methods for real and complex frames of various dimensions in terms of achieved coherence.

II. Method

We rely here on the Gram matrix formulation of (MMC) introduced by Tropp et al. [27]–[29]. Let $G \in \mathbb{F}^{n\times n}$ be the Gram matrix associated with the unit frame $F \in \mathbb{F}^{m\times n}$, i.e., $G_{ij} = \langle f_i, f_j\rangle$ for all (i, j) such that $1 \leqslant i, j \leqslant n$. Without loss of generality, we assume that $\mathbb{F} = \mathbb{C}$ so that

$$G = F^* F, \tag{1}$$

where F^* is the Hermitian conjugate of F. It is readily checked that the Gram matrix G associated with a unit frame

$F \in \mathbb{F}^{m\times n}$ has unit diagonal and belongs to the set of positive-semidefinite matrices of size n with rank at most m

$$\mathbb{S}^+_{m,n} = \{M \in \mathbb{H}^n : M \succcurlyeq 0, \mathrm{rank}(M) \leqslant m\},$$

where $\mathbb{H}^n$ represents the set of $n \times n$ Hermitian matrices. Conversely, for any $G \in \mathbb{S}^+_{m,n}$ with unit diagonal, a unit frame $F \in \mathbb{F}^{m\times n}$ satisfying (1) can be retrieved using the operator

$$\mathcal{F} : \mathbb{S}^+_{m,n} \to \mathbb{C}^{m\times n} : G \mapsto \begin{pmatrix}\mathrm{diag}(\lambda_1, \cdots, \lambda_m)^{\frac{1}{2}} & 0\end{pmatrix} V^*,$$

where $G = V\,\mathrm{diag}(\lambda_1, \cdots, \lambda_m, 0, \cdots, 0)V^*$ is an eigenvalue decomposition with $\lambda_1 \geqslant \cdots \geqslant \lambda_m \geqslant 0$. Note that the mutual coherence $\mu(F)$ can be computed from the Gram matrix G by the function

$$\tilde{\mu} : \mathbb{S}^+_{m,n} \to [0, 1] : G \mapsto \max_{1\leqslant i\neq j\leqslant n} |G_{ij}|.$$

These observations are used in [27] to reformulate (MMC) as an optimization problem over the set $\mathbb{S}^+_{m,n}$:

$$\mu^{\mathbb{F}}_{m,n} = \min_{G\in\mathbb{S}^+_{m,n}} \tilde{\mu}(G) \qquad \text{s.t. } G_{ii} = 1,\ 1 \leqslant i \leqslant n.$$

This minimax objective can be replaced by introducing a new variable $t \geqslant 0$ such that $|G_{ij}| \leqslant t$ for all off-diagonal entries, i.e., these entries belong to the complex unit disk of radius t. These new constraints on G can be written jointly with the unit diagonal constraint as $G \in \mathcal{C}_n(t)$, with

$$\mathcal{C}_n(t) = \{M \in \mathbb{H}^n : M_{ii} = 1,\ \forall i\ ; |M_{ij}| \leqslant t,\ \forall i \neq j\}.$$

The (MMC) problem is thus equivalent to

$$\mu^{\mathbb{F}}_{m,n} = \min_{G\in\mathbb{H}^n, t\geqslant 0} t \quad \text{s.t.} \quad G \in \mathbb{S}^+_{m,n}, G \in \mathcal{C}_n(t). \tag{GMMC}$$

This formulation calls for a bi-level optimization framework where t is the smallest value for which the inner problem

$$\text{Find } G \in \mathbb{H}^n \qquad \text{s.t.} \quad G \in \mathbb{S}^+_{m,n} \cap \mathcal{C}_n(t), \tag{I-t}$$

is feasible. As t represents a mutual coherence, its search interval can be reduced to $[\underline{\mu}^{\mathbb{F}}_{m,n}, 1]$, where $\underline{\mu}^{\mathbb{F}}_{m,n}$ is the largest known lower bound on the mutual coherence for the dimensions-field triplet $(m, n, \mathbb{F})$.

Our Targeted coherence for Accelerated Alternating Projections (TAAP) algorithm is described in Algorithm 1. The feasibility problem I-t is solved by Alternating Projections (AP), similarly to [27]–[29], [32] . For $k \geqslant 1$, the AP iteration reads

$$G_k = \mathcal{P}_{\mathbb{S}^+_{m,n}} \left(\mathcal{P}_{\mathcal{C}_n(t)}(G_{k-1})\right), \tag{2}$$

with $\mathcal{P}_{\mathbb{S}^+_{m,n}}$ and $\mathcal{P}_{\mathcal{C}_n(t)}$ orthogonal projections on $\mathbb{S}^+_{m,n}$ and $\mathcal{C}_n(t)$ respectively, whose expressions are recalled in the two next lemmas.

Lemma II.1 (Projection on $\mathbb{S}^+_{m,n}$). *Let $M \in \mathbb{H}^n$ have an eigendecomposition $M = V\Lambda V^*$, where $\Lambda = \mathrm{diag}(\lambda_1, \cdots, \lambda_n)$, with $\lambda_1 \geqslant \cdots \geqslant \lambda_n$. Then,*

$$\mathcal{P}_{\mathbb{S}^+_{m,n}}(M) = V\,\mathrm{diag}\left((\lambda_1)_+, \cdots, (\lambda_m)_+, 0, \cdots, 0\right) V^*$$

is an orthogonal projection of M on $\mathbb{S}^+_{m,n}$, where $x_+ = \max\{x, 0\}$. This projection is unique iff $\lambda_m > \lambda_{m+1}$.

Proof. This is an immediate consequence of the KKT conditions; see the proof of [27, Proposition 2.3], omitting the trace constraint $\sum_{i=1}^n \lambda_i = n$. □

Lemma II.2 (Projection on $\mathcal{C}_n(t)$). *[27, Proposition 3.1] Let $M \in \mathbb{H}^n$ and $t \geqslant 0$. The projection of M on $\mathcal{C}_n(t)$ is unique and given by:*

$$\left(\mathcal{P}_{\mathcal{C}_n(t)}(M)\right)_{ij} = \begin{cases} 1 & \text{if } i = j, \\ \min\left\{1, \frac{t}{|M_{ij}|}\right\} M_{ij} & \text{if } i \neq j. \end{cases}$$

Building on the analogy between AP and proximal gradient descent (PGD) [33], we define a proximal reformulation of (I-t), with $\mathbb{I}_S$ the indicator function of a set S:

$$\min_{G\in\mathbb{H}^n} \frac{1}{2} \left\|G - \mathcal{P}_{\mathcal{C}_n(t)}(G)\right\|^2_{\mathrm{F}} + \mathbb{I}_{\mathbb{S}^+_{m,n}}(G), \tag{pI-t}$$

which we address using Accelerated Alternating Projections (AAP), incorporating a momentum-based acceleration mechanism proposed by Beck and Teboulle [34], leading to the update rules

$$c_k = \frac{1}{2}\sqrt{4c^2_{k-1} + 1} + \frac{1}{2}, \tag{3}$$

$$Y_k = G_{k-1} + \frac{c_{k-1} - 1}{c_k}(G_{k-1} - G_{k-2}), \tag{4}$$

$$G_k = \mathcal{P}_{\mathbb{S}^+_{m,n}} \left(\mathcal{P}_{\mathcal{C}_n(t)}(Y_k)\right). \tag{5}$$

Despite the nonconvexity of (pI-t) (it is readily checked that the set $\mathbb{S}^+_{m,n}$ is nonconvex), we demonstrate in Section III that this accelerated scheme leads to major computational improvements in practice. The objective can also be shown to satisfy central properties for the convergence of first-order proximal methods [35]–[37]. On the one hand, it verifies the Kurdyka-Łojasiewicz (KL) property since the sets $\mathbb{S}^+_{m,n}$ and $\mathcal{C}_n$ are semi-algebraic [38]. On the other hand, the differentiable part is provably convex and has 1-Lipschitz gradient [33]. Finally, $\mathcal{C}_n(t)$ and a subset of $\mathbb{S}^+_{m,n}$ are known to satisfy conditions sufficient for the convergence of AP [32]. This motivated our choice to resort on AP (and AAP) in this work, though to our knowledge no existing convergence analysis directly applies to our setting.

We then present our *coherence targeting scheme* to progressively update the parameter t in (GMMC). This scheme exploits the lower bound $\underline{\mu}^{\mathbb{F}}_{m,n}$ on the mutual coherence. We write l the search interval *length*, i.e., the gap between the best coherence found by the algorithm so far (written μ_{best}) and the current target coherence t. In case the feasibility problem (I-t) is solved successfully, i.e., the AAP algorithm returns a Gram matrix having mutual coherence (written μ_{AAP}) within a given relative tolerance of the target t, l is increased by a factor $\beta > 1$, so that the new target coherence becomes

$$t = \max\left\{\underline{\mu}^{\mathbb{F}}_{m,n}, \mu_{\text{AAP}} - \beta l\right\}, \tag{6}$$

where the *max* operator ensures that the target remains larger than $\underline{\mu}^{\mathbb{F}}_{m,n}$, and μ_{best} is reduced to μ_{AAP}. In case of failure, the interval l is shrunk to try more conservative target values:

$$t = \max\left\{\underline{\mu}^{\mathbb{F}}_{m,n}, \mu_{\text{AAP}} - \frac{l}{\beta}\right\}. \tag{7}$$

Failure of AAP means that no improvement in terms of mutual coherence larger than $\varepsilon_p l$ was made over the last N_p iterations. We will show in Section III that tuning N_p, a.k.a. the *perseverance* hyperparameter, allows to balance the computational cost against the final coherence of the frame.

Let us finally mention that a post-processing step is required to normalize the Gram matrix $G_{\text{AAP}} \in \mathbb{S}^+_{m,n}$ to G_{best} in line 22 of Algorithm 1. The following similarity transformation is thus applied on G_{AAP}, where $\operatorname{Diag}(G)$ denotes the matrix G with off-diagonal entries put at zero:

$$\mathcal{N} : \mathbb{S}^+_{m,n} \to \mathbb{S}^+_{m,n} : G \mapsto \operatorname{Diag}(G)^{-\frac{1}{2}} G \operatorname{Diag}(G)^{-\frac{1}{2}},$$

which ensures that $G_{\text{best}} \in \mathbb{S}^+_{m,n}$ by Sylvester's law of inertia and that G_{best} has unit diagonal. The operation is equivalent to normalizing the columns of the frame associated with G_{AAP}.

Algorithm 1 TAAP for Grassmannian frame computation

Input: triplet $(m, n, \mathbb{F})$, initial unit frame $F_0 \in \mathbb{F}^{m\times n}$, hyperparameters β, N_{budg}, τ, N_p, ε_p, ε_s
Output: best unit frame $F_{\text{best}} \in \mathbb{F}^{m\times n}$ with coherence μ_{best}

1: $N_{\text{tot}} = 0$
2: $G_{\text{best}} = F_0^* F_0$, $\mu_{\text{best}} = \mu(F_0)$
3: $t = \underline{\mu}^{\mathbb{F}}_{m,n}$, $l = \mu_{\text{best}} - t$
4: **while not** ($l < \tau$ **or** $N_{\text{tot}} > N_{\text{budg}}$) **do**
5:   **/ Start Accelerated Alternating Projections (AAP) */*
6:   $G_{\text{AAP}} = G_{\text{best}}$, $\mu_{\text{AAP}} = \mu_{\text{best}}$, $k_{\text{AAP}} = 0$
7:   $c_0 = 1$, $G_{-1} = G_{\text{AAP}}$, $G_0 = G_{\text{AAP}}$, $k = 1$
8:   **while not** ($\mu_{\text{AAP}} - t < \varepsilon_s l$ **or** $k - k_{\text{AAP}} > N_p$) **do**
9:     Compute c_k, Y_k, G_k by (3), (4), (5)
10:     $\mu_k = \tilde{\mu}(\mathcal{N}(G_k))$
11:     **if** $\mu_{\text{AAP}} - \mu_k > \varepsilon_p l$ **then**
12:       $G_{\text{AAP}} = G_k$, $\mu_{\text{AAP}} = \mu_k$, $k_{\text{AAP}} = k$
13:     **end if**
14:     $k = k + 1$, $N_{\text{tot}} = N_{\text{tot}} + 1$
15:   **end while**
16:   **/ End AAP */*
17:   **if** $\mu_{\text{AAP}} - t < \varepsilon_s l$ **then**
18:     Compute t according to (6)
19:   **else if** $k - k_{\text{AAP}} > N_p$ **then**
20:     Compute t according to (7)
21:   **end if**
22:   $G_{\text{best}} = \mathcal{N}(G_{\text{AAP}})$, $\mu_{\text{best}} = \mu_{\text{AAP}}$, $l = \mu_{\text{best}} - t$
23: **end while**
24: $F_{\text{best}} = \mathcal{F}(G_{\text{best}})$

III. Numerical results

Figure 1 shows a typical run of our TAAP algorithm. First, the coherence decreases quickly while targeting the lower bound $\underline{\mu}^{\mathbb{F}}_{m,n}$. When AAP fails to solve (I-t) for the current target coherence, the target starts increasing due to (7) and the improvements reactivate but at a slower pace. We clearly observe the nested loop structure: the outer loop adjusts the target and the inner loop tries to reach this value with AAP.

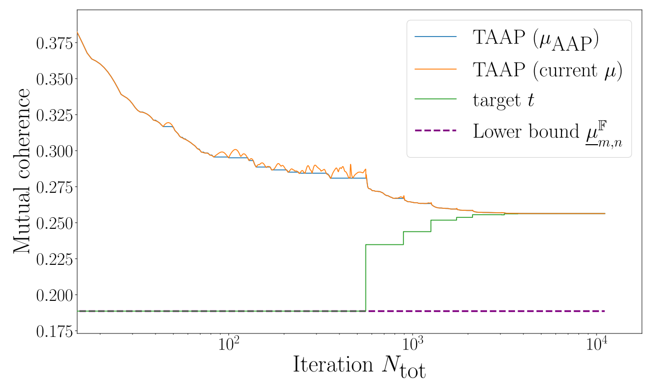

Fig. 1: Evolution of the mutual coherence during a run of TAAP, for the dimensions-field triplet $(30, 1000, \mathbb{C})$.

We compare our TAAP algorithm with IDB [23], TELET [4] and CPM [24], which are state-of-the-art methods respectively in the real and complex settings. Table I provides the final coherence achieved by these three algorithms for different frame dimensions and shapes. The values provided in Table I for TAAP correspond to the best frame over 3 runs when $n < 1000$ and 1 run when $n \geqslant 1000$. The values for the other methods come from their respective original papers [4], [23], [24]. Each TAAP run is initialized with a frame with Gaussian entries, normalized columnwise. The *perseverance* hyperparameter was set to $N_p = 100$ to approximately match the computation budget of IDB reported in its paper [23]. Note that lower coherence can be achieved with higher N_p. Other hyperparameters were chosen as $\varepsilon_p = 10^{-3}$, $\varepsilon_s = 10^{-1}$, $\beta = 2$, $\tau = 10^{-6}$ and $N_{\text{budg}} = 10^5$. Experiments were conducted on a laptop with i7 processor (10 cores, 1.7GHz) and 16GB RAM. Codes can be found here: https://github.com/bastmas6/taap.

Table II compares TAAP with the best packings obtained on the reference leaderboards of the community for small-dimensional frames: [39] for real frames and [40] for complex frames. The table presents, for each field, the number of dimensions (m, n) considered in the leaderboards (column "Total"). Among them, we report the number of cases for which the coherence obtained by our algorithm outperforms the best algorithm of the leaderboard (column "Better"), is equal to the best value on the leaderboard (column "Equal") within a tolerance of 10^{-6}, or reaches the best lower bound known on the mutual coherence for the corresponding triplet ("optimal", numbers in brackets) within this tolerance.

Tables I and II show that our TAAP algorithm often achieves lower coherence than existing methods, especially for weakly overcomplete (when m is close to n) and complex frames. They also illustrate the gap between lower bounds and the lowest mutual coherence found numerically; this difference is

m	n	$\underline{\mu}^{\mathbb{R}}_{m,n}$	IDB	TAAP	$\underline{\mu}^{\mathbb{C}}_{m,n}$	Other	TAAP
25	800	0.2871	0.3654	**0.3646**	0.2171	0.3143	**0.2807**
25	1000	0.2972	**0.3829**	**0.3829**	0.2308	0.3292	**0.2981**
30	1000	0.2564	**0.3315**	0.3319	0.1886	0.2962	**0.2563**
50	1000	0.1379	0.2224	**0.2195**	0.1379	0.2229	**0.1782**
40	1200	0.1985	0.2747	**0.2740**	0.1555	0.2745	**0.2171**
20	5000	0.3645	**0.5500**	0.5576	0.3027	0.6124	**0.4415**
64	128	0.0887	0.0962	**0.0957**	0.0887	0.0888	**0.0887**
64	256	0.1085	0.1295	**0.1279**	0.1084	0.1118	**0.1110**
64	640	0.1187	0.1675	**0.1670**	0.1187	0.1395	**0.1377**
64	960	0.1208	0.1843	**0.1838**	0.1208	0.1521	**0.1493**
64	1600	0.1225	0.2064	**0.2042**	0.1225	0.1742	**0.1655**
64	2880	0.1541	0.2325	**0.2322**	0.1236	0.1963	**0.1837**
64	4096	0.1740	**0.2488**	0.2491	0.1240	0.2098	**0.1935**
50	60	0.0585	0.0626	**0.0623**	0.0582	-	**0.0586**
90	100	0.0343	0.0374	**0.0371**	0.0335	-	**0.0341**
200	210	0.0160	0.0176	**0.0175**	0.0157	-	**0.0160**
500	550	0.0135	0.0151	**0.0150**	0.0135	-	**0.0138**
700	710	0.0047	**0.0053**	**0.0053**	0.0046	-	**0.0047**
900	1100	0.0142	0.0155	**0.0154**	0.0142	-	**0.0144**
2000	2500	0.0100	0.0109	**0.0107**	0.0100	-	**0.0101**

TABLE I: Mutual coherence for real and complex frames, following tables from [23], [4] and [24]. "Other" stands for TELET for the first block and CPM for the second (no previous results exist for the third block).

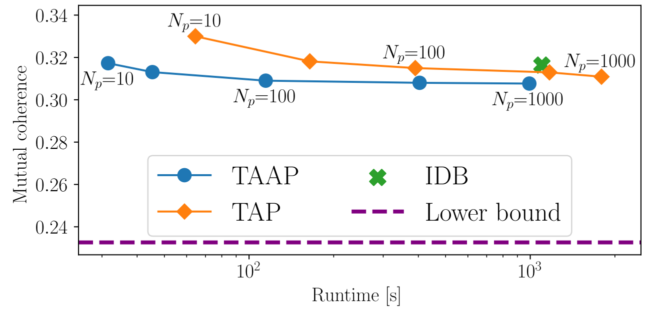

(a) Strongly overcomplete frame $(20, 230, \mathbb{R})$

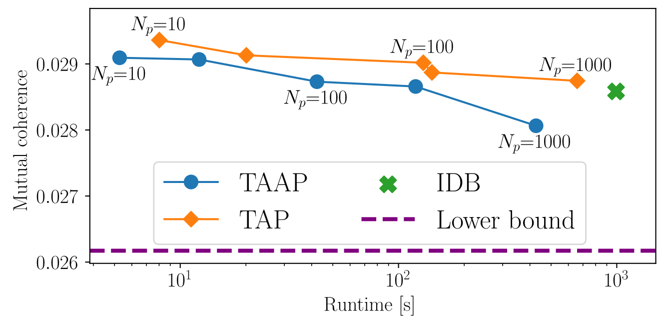

(b) Weakly overcomplete frame $(120, 130, \mathbb{R})$

Fig. 2: Mutual coherence-runtime graph for different frame dimensions. The displayed values correspond to the best of 5 runs per method and per N_p value.

more pronounced for real frames and for frames with $m \ll n$, which suggests that tighter bounds can be found and/or that numerical methods can be improved in these regimes.

Field	Better (optimal)	Equal (optimal)	Total
$\mathbb{R}$	**29** (0)	**212** (81)	615
$\mathbb{C}$	**76** (0)	**112** (41)	267

TABLE II: Comparison with mutual coherence leaderboards.

Figure 2 compares TAAP with IDB (re-implemented in Python for fair comparison) for weakly and strongly overcomplete frames. In both scenarios, TAAP outperforms IDB in terms of final coherence and computation time. The coherence targeting scheme of TAAP likely contributes to the improvement over IDB and its bisection-based scheme. While IDB restarts from scratch when the target is updated, TAAP continues from the previous best frame, thus leveraging the past work. Figure 2 also illustrates the benefits of performance of the acceleration scheme integrated into the alternating projections: TAAP improves on TAP (Targeted coherence with Alternating Projections) for coherence, while stopping earlier. Note that TAP denotes the non-accelerated version of our algorithm (line 9 of Algorithm 1 is replaced with the classical Alternating projections (2)).

Finally, Figure 2 shows the role of the *perseverance* hyperparameter N_p, which represents the number of iterations allowed without improvement before the termination of AAP. A more *perseverent* algorithm, i.e., with large N_p, will try for a longer period to get past bad feasible regions such as saddle points, local minima or plateaus, which are caused by the nonconvexity of the problem. Therefore, N_p acts as a trade-off parameter between runtime and frame quality: small values of N_p (≈ 10) enforce quick termination of the algorithm with modest coherence quality, while large values of N_p (≈ 1000) permit to achieve high-quality frames, beating state-of-the-art low-coherence results almost any time, at the cost of (much) longer runtimes, as demonstrated on Figure 2. Our experiments indicate that $N_p \approx 100$ is a good trade-off.

IV. Discussion

We propose a novel algorithm to solve (MMC) for any dimensions in real and complex settings. Arguably the main limitation of TAAP is the cost of the projection on $\mathbb{S}^+_{m,n}$, due to the eigendecomposition of the $n \times n$ Gram matrix G, whose cost scales as $\mathcal{O}(n^3)$. In comparison, frame-based methods typically show $\mathcal{O}(mn^2)$ complexity [24]. This difference hinders the competitiveness of TAAP for strongly overcomplete dimensions ($m \ll n$), but our method excels in the weakly overcomplete regime, i.e., when $m \approx n$, regarding runtime as well as coherence. Our implementation mitigates this bottleneck by using a truncated eigendecomposition of G [41], [42] since, by Lemma II.1, the projection only requires the m dominant eigenvalues and eigenvectors. Two other avenues worth exploring are randomized eigenvalue algorithms [43] and an extension of our method to apply projections directly on the frame, without any work on the Gram matrix.

References

[1] T. Strohmer and R. W. Heath, “Grassmannian frames with applications to coding and communication,” *Applied and Computational Harmonic Analysis*, vol. 14, no. 3, pp. 257–275, 2003.

[2] B. Tahir, S. Schwarz, and M. Rupp, “Constructing Grassmannian Frames by an Iterative Collision-Based Packing,” *IEEE Signal Processing Letters*, vol. 26, no. 7, pp. 1056–1060, 2019.

[3] D. Donoho, M. Elad, and V. Temlyakov, “Stable recovery of sparse overcomplete representations in the presence of noise,” *IEEE Transactions on Information Theory*, vol. 52, no. 1, pp. 6–18, 2006.

[4] R. Jyothi and P. Babu, “TELET: A monotonic algorithm to design large dimensional equiangular tight frames for applications in compressed sensing,” *Signal Processing*, vol. 195, p. 108503, 2022.

[5] J. Jasper, E. J. King, and D. G. Mixon, “Game of Sloanes: best known packings in complex projective space,” vol. 11138, pp. 416–425, 2019.

[6] J. M. Renes, R. Blume-Kohout, A. J. Scott, and C. M. Caves, “Symmetric informationally complete quantum measurements,” *Journal of Mathematical Physics*, vol. 45, no. 6, pp. 2171–2180, 2004.

[7] M. Appleby, T.-Y. Chien, S. Flammia, and S. Waldron, “Constructing exact symmetric informationally complete measurements from numerical solutions,” *Journal of Physics A: Mathematical and Theoretical*, vol. 51, no. 16, p. 165302, 2018.

[8] I. Bengtsson, M. Grassl, and G. McConnell, “SIC-POVMs from Stark Units: Dimensions n^2+3=4p, p prime,” 2024. [Online]. Available: http://arxiv.org/abs/2403.02872

[9] W. U. Bajwa, R. Calderbank, and D. G. Mixon, “Two are better than one: Fundamental parameters of frame coherence,” *Applied and Computational Harmonic Analysis*, vol. 33, no. 1, pp. 58–78, 2012.

[10] P. Xia, S. Zhou, and G. Giannakis, “Achieving the Welch bound with difference sets,” *IEEE Transactions on Information Theory*, vol. 51, no. 5, pp. 1900–1907, 2005.

[11] M. Fickus, J. Jasper, and D. G. Mixon, “Packings in Real Projective Spaces,” *SIAM Journal on Applied Algebra and Geometry*, vol. 2, no. 3, pp. 377–409, 2018.

[12] L. Welch, “Lower bounds on the maximum cross correlation of signals,” *IEEE Transactions on Information Theory*, vol. 20, no. 3, pp. 397–399, 1974.

[13] M. Fickus and D. G. Mixon, “Tables of the existence of equiangular tight frames,” 2016. [Online]. Available: http://arxiv.org/abs/1504.00253

[14] J. J. Benedetto and J. D. Kolesar, “Geometric Properties of Grassmannian Frames for R2 and R3,” *EURASIP Journal on Advances in Signal Processing*, vol. 2006, no. 1, pp. 1–17, 2006.

[15] H. Cohn and J. Woo, “Three-point bounds for energy minimization,” *Journal of the American Mathematical Society*, vol. 25, no. 4, pp. 929–958, 2012.

[16] D. G. Mixon and H. Parshall, “The Optimal Packing of Eight Points in the Real Projective Plane,” *Experimental Mathematics*, vol. 31, no. 2, pp. 474–485, 2022.

[17] C. Lu, H. Li, and Z. Lin, “Optimized projections for compressed sensing via direct mutual coherence minimization,” *Signal Processing*, vol. 151, pp. 45–55, 2018.

[18] A. Medra and T. N. Davidson, “Flexible Codebook Design for Limited Feedback Systems Via Sequential Smooth Optimization on the Grassmannian Manifold,” *IEEE Transactions on Signal Processing*, vol. 62, no. 5, pp. 1305–1318, 2014.

[19] J. Park, C. Saltijeral, and M. Zhong, “Grassmannian packings: Trust-region stochastic tuning for matrix incoherence,” pp. 1–6, 2022.

[20] C. Rusu and N. González-Prelcic, “Designing Incoherent Frames Through Convex Techniques for Optimized Compressed Sensing,” *IEEE Transactions on Signal Processing*, vol. 64, no. 9, pp. 2334–2344, 2016.

[21] R. Jyothi, P. Babu, and P. Stoica, “Design of High-Dimensional Grassmannian Frames via Block Minorization Maximization,” *IEEE Communications Letters*, vol. 25, no. 11, pp. 3624–3628, 2021.

[22] J. Kwon and N. Y. Yu, “Finding Subsampling Index Sets for Kronecker Product of Unitary Matrices for Incoherent Tight Frames,” *Applied Sciences*, vol. 12, no. 21, p. 11055, 2022.

[23] D. C. Ilie-Ablachim and B. Dumitrescu, “Incoherent frames design and dictionary learning using a distance barrier,” *Signal Processing*, vol. 209, p. 109019, 2023.

[24] F. Tong, D. Zhao, C. Chen, and L. Li, “Coherence-penalty minimization method for incoherent unit-norm tight frame design,” *Signal Processing*, vol. 205, p. 108864, 2023.

[25] D. Cuevas, C. Beltran, I. Santamaria, V. Tucek, and G. Peters, “A Fast Algorithm for Designing Grassmannian Constellations,” pp. 1–6, 2021.

[26] H. E. A. Laue and W. P. du Plessis, “A Coherence-Based Algorithm for Optimizing Rank-1 Grassmannian Codebooks,” *IEEE Signal Processing Letters*, vol. 24, no. 6, pp. 823–827, 2017.

[27] J. A. Tropp, “Constructing packings in projective spaces and Grassmannian spaces via alternating projection,” *ICES Report*, pp. 04–23, 2004.

[28] J. Tropp, I. Dhillon, R. Heath, and T. Strohmer, “Designing structured tight frames via an alternating projection method,” *IEEE Transactions on Information Theory*, vol. 51, no. 1, pp. 188–209, 2005.

[29] I. S. Dhillon, J. R. W. Heath, T. Strohmer, and J. A. Tropp, “Constructing Packings in Grassmannian Manifolds via Alternating Projection,” *Experimental Mathematics*, vol. 17, no. 1, pp. 9–35, 2008.

[30] M. Sadeghi and M. Babaie-Zadeh, “Incoherent Unit-Norm Frame Design via an Alternating Minimization Penalty Method,” *IEEE Signal Processing Letters*, vol. 24, no. 1, pp. 32–36, 2017.

[31] F. Tong, D. Zhao, X. Li, and L. Li, “Designing incoherent unit norm tight frames via block coordinate descent-based alternating projection,” *Applied Mathematics and Computation*, vol. 474, p. 128687, 2024.

[32] Z. Zhu and X. Li, “Convergence Analysis of Alternating Projection Method for Nonconvex Sets,” 2019. [Online]. Available: http://arxiv.org/abs/1802.03889

[33] J. Bolte, T. P. Nguyen, J. Peypouquet, and B. W. Suter, “From error bounds to the complexity of first-order descent methods for convex functions,” *Mathematical Programming*, vol. 165, no. 2, pp. 471–507, 2017.

[34] A. Beck and M. Teboulle, “Fast Gradient-Based Algorithms for Constrained Total Variation Image Denoising and Deblurring Problems,” *IEEE Transactions on Image Processing*, vol. 18, no. 11, pp. 2419–2434, 2009.

[35] H. Li and Z. Lin, “Accelerated Proximal Gradient Methods for Nonconvex Programming,” vol. 28, 2015.

[36] Q. Li, Y. Zhou, Y. Liang, and P. K. Varshney, “Convergence Analysis of Proximal Gradient with Momentum for Nonconvex Optimization,” pp. 2111–2119, 2017.

[37] X. Jia, C. Kanzow, and P. Mehlitz, “Convergence Analysis of the Proximal Gradient Method in the Presence of the Kurdyka–Łojasiewicz Property Without Global Lipschitz Assumptions,” *SIAM Journal on Optimization*, vol. 33, no. 4, pp. 3038–3056, 2023.

[38] J. Bolte, S. Sabach, and M. Teboulle, “Proximal alternating linearized minimization for nonconvex and nonsmooth problems,” *Mathematical Programming*, vol. 146, no. 1, pp. 459–494, 2014.

[39] N. J. A. Sloane, “Table of Grassmannian Packings.” [Online]. Available: http://neilsloane.com/grass/grassTab.html

[40] Emily J. King, “Game of Sloanes.” [Online]. Available: https://www.math.colostate.edu/~king/GameofSloanes.html#leader

[41] I. S. Dhillon and B. N. Parlett, “Orthogonal Eigenvectors and Relative Gaps,” *SIAM Journal on Matrix Analysis and Applications*, vol. 25, no. 3, pp. 858–899, 2003.

[42] D. S. Watkins, *Fundamentals of Matrix Computations*. John Wiley & Sons, 2004.

[43] N. Halko, P. G. Martinsson, and J. A. Tropp, “Finding Structure with Randomness: Probabilistic Algorithms for Constructing Approximate Matrix Decompositions,” *SIAM Review*, vol. 53, no. 2, pp. 217–288, 2011.